

Ion partitioning between brines and ion exchange polymers

Michele Galizia^a, Gerald S. Manning^b, Donald R. Paul^c, Benny D. Freeman^{c,d,*}

^a School of Chemical, Biological and Materials Engineering, 100E. Boyd Street, 73019, Norman, The University of Oklahoma, USA

^b Department of Chemistry and Chemical Biology, 610 Taylor Road, 08854-8087, Piscataway, Rutgers University, NJ, USA

^c John J. McKetta Jr. Department of Chemical Engineering, The University of Texas at Austin, 200 E. Dean Keeton Street, 78712, Austin, USA

^d Center for Energy and Environmental Resources, The University of Texas at Austin, 10100 Burnet Road, Building 133 (CEER), 78758, Austin, USA

HIGHLIGHTS

- Ion partitioning between brines and IEMs is described by the ideal Donnan model.
- Ion activity coefficients in the membrane and in solution are equal at high salt concentration.
- Sulfonated polystyrene behaves like an uncharged polymer in CaCl_2 brines.

ARTICLE INFO

Keywords:

Ion exchange polymers
Brines
Donnan model

ABSTRACT

Quantitative failure of the ideal Donnan model to predict ion partitioning between relatively dilute electrolyte aqueous solutions and ion exchange polymers arises from neglecting non-ideal behavior of ions. Hypothetically, when a water swollen, charged polymer is equilibrated with concentrated salt solutions, most of the fixed charge groups are neutralized by sorbed counter-ions, which can screen electrostatic effects and create, in the membrane, an environment thermodynamically similar to that experienced by ions in the external electrolyte solution. In this study, a combined experimental and theoretical approach was used to test this hypothesis. A fundamental study of ion partitioning between a cation exchange membrane based on cross-linked poly(p-styrene sulfonate-co-divinylbenzene) and NaCl and CaCl_2 concentrated brines is presented. At high electrolyte concentrations, the experimentally measured ion activity coefficients in the membrane match those in the contiguous external solution, and the ideal Donnan model provides an accurate prediction of co-ion and counter-ion concentrations in the polymer. This physical picture was further confirmed by the recently developed Manning-Donnan model.

1. Introduction and background

Ion exchange membranes (IEMs) have attracted interest for electrodialysis (ED), reverse electrodialysis (RED), reverse osmosis (RO), pressure retarded osmosis (PRO), fuel cells, batteries and artificial photosynthesis [1–5]. IEMs are often synthesized from cross-linked, hydrocarbon-based polymers bearing ionizable functional groups on their backbone [1,6]. Covalent cross-linking controls polymer swelling and prevents dissolution of the IEM in the contiguous aqueous electrolyte solution [7]. Negatively charged polymers exhibiting selective permeability for cations are called cation exchange membranes (CEMs). Positively charged polymers, selectively permeable to anions, are called anion exchange membranes (AEMs) [1,6].

The extent to which a polymer is charged is often quantified by the ion exchange capacity (IEC), which is the milliequivalents of fixed

charge on the polymer chains per gram of dry polymer [1,6,7]. However, the concentration of fixed charge groups, expressed as mols of fixed charge group per unit volume of water sorbed by the ion exchange polymer, $C_A^{m,w}$, is more appropriate for describing the charge density experienced by ions sorbed into IEMs equilibrated with electrolyte solutions [7]. The presence of these charge groups strongly influences ion sorption and transport in IEMs [7–10].

In this study, monovalent and divalent ion sorption from concentrated brines in a commercial cation exchange membrane based on cross-linked poly(p-styrene sulfonate-co-divinylbenzene), as well as in a model uncharged hydrogel, cross-linked poly(ethylene glycol diacrylate) (XLPEGDA), is investigated and interpreted within the framework of the Donnan [8] and Donnan-Manning models [9]. This topic is of practical interest, for example, in ED and RED, where IEMs can contact highly concentrated brines [1]. Moreover, IEM behavior in

* Corresponding author. John J. McKetta Jr. Department of Chemical Engineering, 200 E. Dean Keeton Street, 78712, Austin, USA.

E-mail address: freeman@che.utexas.edu (B.D. Freeman).

concentrated electrolyte solutions provides essential information to optimize PRO technology, which uses such brines to produce energy. In PRO applications, membranes face brines whose NaCl concentration can be 9% wt (1.5 mol/L) or higher. The vast majority of ion sorption and transport studies in IEMs have focused on dilute electrolyte solutions (< 1 mol/L). To the best of our knowledge, this is the first fundamental study of ion partitioning between IEMs and concentrated brines.

According to the solution-diffusion model [11], ion sorption significantly influences ion transport in dense polymers [7]. When a IEM is equilibrated with an electrolyte solution, fixed charge groups cannot leave the membrane since they are covalently bound to it. So, a Donnan equilibrium develops between the membrane and the contiguous external solution [8]. Depending on the concentration of fixed charge groups, $C_A^{m,w}$, counter-ion (i.e., ions of opposite charge to the polymer fixed charges) concentration in the membrane may be 2–3 orders of magnitude higher than that in the contiguous external solution at low external electrolyte concentrations [9,10]. To ensure membrane electro-neutrality, an equivalent molar amount of counter-ions sorb into the IEM to balance the fixed charge groups on the IEM. Additionally, any sorbed co-ions (i.e., ions of the same charge as that of the polymer fixed charge groups) require an equivalent molar amount of mobile counter ions to sorb into the IEM. In contrast, co-ion concentration in the membrane can be significantly lower than in the external solution at low external electrolyte concentrations [9,10]. Due to this unequal distribution of ions between the membrane and solution, an electrical potential, called the Donnan potential, develops at the polymer-solution interface. It acts to inhibit co-ion sorption in the membrane and counter-ion desorption from the membrane [8]. This phenomenon is referred to as Donnan exclusion [8].

Ion partition equilibrium between an aqueous electrolyte solution containing a salt $M_{\nu_M}^{z_M} X_{\nu_X}^{z_X}$ and an IEM requires the electrochemical potential of each ion in the membrane phase (i.e., $\bar{\mu}_i^m$) to be equal to its electrochemical potential in the contiguous electrolyte solution (i.e., $\bar{\mu}_i^s$) [6,9,10]. Superscripts m and s stand for the membrane and contiguous electrolyte solution, respectively. The equilibrium condition is commonly expressed by equating the sum of the electrochemical potentials of all ions in the membrane phase to the sum of the electrochemical potentials of all ions in the solution phase [1,7,10]:

$$\sum_i \nu_i \bar{\mu}_i^m = \sum_i \nu_i \bar{\mu}_i^s \quad (1)$$

where ν_M and ν_X are the stoichiometric coefficients of the cation and anion, respectively. Plugging the expression for the electrochemical potential into Eq. (1) gives [10]:

$$(\gamma_M^m C_M^{m,w})^{\nu_M} (\gamma_X^m C_X^{m,w})^{\nu_X} = (\gamma_M^s C_M^s)^{\nu_M} (\gamma_X^s C_X^s)^{\nu_X} \quad (2)$$

where γ_M^m and γ_X^m are the activity coefficients of cations and anions in the membrane, respectively. $C_M^{m,w}$ and $C_X^{m,w}$ are the concentrations of cations and anions in the membrane, respectively, expressed in units of moles of ions per liter of water sorbed in the IEM. The quantities γ_M^s , γ_X^s , C_M^s and C_X^s have the same meaning, but they refer to the external electrolyte solution. The mean salt activity coefficient in the external solution, γ_{MX}^s , is defined as follows [12]:

$$\gamma_{MX}^s = (\nu_M + \nu_X) \sqrt{(\gamma_M^s)^{\nu_M} (\gamma_X^s)^{\nu_X}} \quad (3)$$

In this study, γ_{MX}^s was calculated using the Pitzer model [12].

For a cation exchange membrane bearing sulfonate groups on its backbone, the total charge balance can be written as follows:

$$z_M C_M^{m,w} + z_X C_X^{m,w} = C_A^{m,w} \quad (4)$$

where z_M and z_X are the cation and anion valences, respectively, and the other symbols have the usual meaning. Combining Eq. (4) with Eq. (2) gives an analytic expression for co-ion concentration in the membrane, which is known as the Donnan model [10]. For a monovalent salt, MX , (i.e., when $\nu_M = \nu_X = 1$), the Donnan model gives the

following expression for co-ion (i.e., $C_X^{m,w}$) sorption [9,10]:

$$(C_A^{m,w} + C_X^{m,w}) C_X^{m,w} = \frac{(\gamma_{MX}^s)^2}{\gamma_M^m \gamma_X^m} (C_s^s)^2 \quad (5)$$

where C_s^s represents the salt concentration in the external electrolyte solution. For a divalent salt, MX_2 , (i.e., when $\nu_M = 1$ and $\nu_X = 2$), the Donnan model provides the following expression for co-ion (i.e., $C_X^{m,w}$) sorption [10]:

$$\left(\frac{C_A^{m,w} + C_X^{m,w}}{2} \right) (C_X^{m,w})^2 = \frac{4(\gamma_{MX}^s)^3}{\gamma_M^m (\gamma_X^s)^2} (C_s^s)^3 \quad (6)$$

Eqs. (5) and (6) can be used to calculate ion activity coefficients in the membrane when $C_M^{m,w}$ and $C_X^{m,w}$ are known experimentally [10]. Specifically, for a monovalent salt, MX , Eq. (5) can be re-arranged as follows [10]:

$$\gamma_M^m \gamma_X^m = \frac{(\gamma_{MX}^s C_s^s)^2}{C_M^{m,w} C_X^{m,w}} \quad (7)$$

For a divalent salt, MX_2 , Eq. (6) becomes [10]:

$$(\gamma_M^m)(\gamma_X^m)^2 = \frac{4(\gamma_{MX}^s C_s^s)^3}{(C_M^{m,w})(C_X^{m,w})^2} \quad (8)$$

The ratio of solution-to-membrane ion activity coefficients in Eqs. (5) and (6), Γ , is defined, for monovalent (MX) and divalent salts (MX_2), respectively, as follows [10]:

$$\Gamma = \frac{(\gamma_{MX}^s)^2}{\gamma_M^m \gamma_X^m} \quad (9)$$

$$\Gamma = \frac{4(\gamma_{MX}^s)^3}{(\gamma_M^m)(\gamma_X^m)^2} \quad (10)$$

In the ideal Donnan model, Γ is set equal to one. That is, ion activity coefficients in the membrane are assumed to be equal to those in the external solution, or ion activity coefficients are assumed to be equal to one in both phases [8]. However, when Eqs. (5) and (6) are used to predict co-ion sorption in ion exchange polymers and resins with $\Gamma = 1$, poor quantitative agreement with experimental data is generally observed [9]. The inability of the Donnan model to predict ion sorption in charged polymers is believed to arise from neglecting non-ideal behavior of ions in the membrane [9,10]. Indeed, electrostatic interactions between fixed charge groups and counter-ions lead to strongly non-ideal behavior especially at low electrolyte concentrations (i.e., at low C_s^s) [9,10]. In contrast, when an IEM is soaked in highly concentrated brines (i.e., when C_s^s is similar to or greater than the IEM fixed charge concentration, $C_A^{m,w}$), most of the fixed charges can be screened by sorbed counter-ions, which should render the environment inside the membrane more similar to that in solution.

Recently, Manning counter-ion condensation theory [13], originally developed to describe non-ideality in polyelectrolyte solutions, was used to calculate ion activity coefficients in IEMs. When combined with the Donnan model, the resulting Manning-Donnan model [9] provides improved quantitative prediction of ion sorption in IEMs relative to the ideal Donnan model. The only parameter in Donnan-Manning model is the dimensionless polymer linear charge density, ξ , which is defined as follows [13]:

$$\xi = \frac{\lambda_b}{b} = \frac{e^2}{4\pi\epsilon_0\epsilon kTb} \quad (11)$$

where λ_b is the Bjerrum length, b is the distance between fixed charge groups on the polymer chain, e is the elementary charge (1.6×10^{-19} C), ϵ_0 is the vacuum dielectric constant (8.85×10^{-12} F/m), and ϵ is the dielectric constant of the swollen polymer. Finally, k and T are the Boltzmann constant and the absolute temperature, respectively. ξ can be calculated once the polymer chemical structure and the concentration of fixed charge groups, $C_A^{m,w}$, are known. If ξ is greater than a

critical value ($\xi_{cr} = 1/|z_M|$), counter-ion condensation occurs [9,13]. In this case, some counter-ions do not have enough thermal energy to readily escape from the overlapped electrical fields generated by nearby fixed charge groups, so they are “condensed” on the fixed charge groups. If ξ is less than the critical value, counter-ions have sufficient thermal energy to readily diffuse away from the fixed charge groups, so counter-ion condensation does not occur. In this condition, counter-ions are referred to as “free”. ξ_{cr} is 1 for alkali chlorides (e.g., NaCl) and 0.5 for alkaline earth chlorides (e.g., CaCl_2) [9,10,13,14].

2. Experimental

2.1. Materials

A commercial cation exchange membrane based on cross-linked poly(p-styrene sulfonate-co-divinylbenzene), CR61, was kindly provided by General Electric Power and Water in the sodium counter-ion form.

The ion exchange resin is polymerized into a hydrophobic, non-woven fabric backing which provides mechanical support and does not sorb water and ions [10]. Ion and water sorption data measured for these composite membranes were corrected for the effect of the backing as discussed elsewhere [10]. Selected membrane properties, such as IEC, water uptake (w_u) and fixed charge group concentration ($C_A^{m,w}$), are reported in Table 1 and reflect values of these properties for the ion exchange polymer only, i.e., not including the backing. To verify membrane integrity after soaking in concentrated brines, membrane samples were dyed using a dilute solution (1 g/L) of Erythrosin B in water and observed under an optical microscope. Membrane integrity is an essential condition to measure reliable values of water uptake and ion sorption.

Cross-linked poly(ethylene glycol diacrylate) (XLPEGDA) was chosen as an uncharged model hydrogel for comparison. Dense XLPEGDA films were prepared via UV radical photo-polymerization, as reported previously [7,10]. Poly(ethylene glycol diacrylate) (average $M_n = 575$ g/mol, Sigma-Aldrich, Milwaukee, WI) was mixed with deionized water (25% wt) and 2,2-dimethoxy-2-phenylacetophenone (DMPA, 0.1% wt of the pre-polymerization solution, Sigma-Aldrich, Milwaukee, WI), which served as the photo-initiator. The pre-polymerization solution was then cast between two quartz plates and cross-linked under UV irradiation (wavelength 312 nm) for 3 min at 3 mW/cm² in a UV cross-linker (UVXL-1000, Spectronic Corporation, Westbury, NY). The nascent films, 350 μm thick, were soaked in deionized water for 48 h to remove any impurities and other species not bound to the cross-linked network. Pure liquid water uptake by XLPEGDA is reported in Table 1.

The chemical structures of the polymers under study are shown in Fig. S1 of the Supporting Information.

Sodium chloride (NaCl) and calcium chloride (CaCl_2) were purchased from Sigma Aldrich (Milwaukee, WI, purity > 99.6%) and were used as received. De-ionized water (TOC content < 5.4 ppb, specific

conductivity < 0.055 $\mu\text{S}/\text{cm}$) was generated by a Millipore System (RiOS8, Billerica, MA).

2.2. Membrane conversion

The CR61 membrane, originally supplied in the sodium counter-ion form, was converted to the calcium counter-ion form before measuring ion and water sorption in the presence of CaCl_2 solutions. As received membrane samples were soaked in a 0.01 mol/L aqueous CaCl_2 solution, and Ca^{2+} ions were allowed to ion exchange with Na^+ ions. Details regarding the conversion protocol were reported previously by Galizia et al. [10]. Following conversion, membranes were soaked in deionized water for 48 h to remove any sorbed mobile ions [10].

2.3. Water uptake

Water uptake was measured at ambient temperature. Circular membrane samples (diameter = 2.5 cm) in the appropriate counter-ion form were soaked in pure de-ionized water and in NaCl and CaCl_2 aqueous solutions, whose concentrations ranged from 0.01 mol/L to 5 mol/L and 6 mol/L, respectively, until reaching equilibrium. After 48 h, the membranes were removed from the salt solutions and quickly wiped with a clean paper towel to remove excess solution on their surface. Membrane wet mass (m_w) was measured using an analytical balance (Mettler Toledo, precision 10^{-4} g). The membranes were then dried in a vacuum oven at ambient temperature until reaching a constant dry mass (m_d). Water sorption in the ion exchange polymer, w_u , was calculated by subtracting the mass of the porous backing from the total mass of the composite membrane [10]. Since the backing material does not sorb water, water uptake by the ion exchange polymer was calculated as follows [10]:

$$w_u = \frac{m_w - m_d}{m_d - m'A} \quad (12)$$

where A is the membrane area, and m' is the mass of backing per unit area (15.6 mg/cm²) [10]. Finally, water volume fraction was estimated assuming volume additivity:

$$\phi_w = \frac{w_u}{w_u + \rho_w/\rho_p} \quad (13)$$

where ρ_w is the density of pure liquid water at ambient temperature (1.0 g/cm³), and ρ_p is the experimentally determined density of the dry ion exchange polymer (i.e., 1.21 g/cm³) [9]. A similar protocol was used to estimate water sorption in XLPEGDA.

2.4. Ion sorption

In this study, anion and cation sorption in CR61 was measured following procedures reported elsewhere [10,15]. The experimental protocol is briefly summarized here. Circular membrane samples, whose diameters ranged from 2.2 to 4.3 cm, in the appropriate counter-ion form, were soaked in deionized water for 48 h. Then, the swollen

Table 1
Selected properties of CR61 and XLPEGDA.

	w_u [g(water)/g(dry polymer)]	ϕ_w	IEC [meq/g(dry polymer)]	$C_A^{m,w}$ [(mol charged groups)/L (sorbed water)]
CR61	0.828 \pm 0.03 ^a	0.501 \pm 0.01 ^a	2.2 (minimum) ^c	3.0 \pm 0.1 ^d
XLPEGDA	0.576 \pm 0.004 ^b	0.409 \pm 0.002 ^b	0	0

^a This value refers to the original membrane in the Na^+ counter-ion form. w_u was adjusted by subtracting the contribution of the backing, as described in Ref. [10], to give the water uptake in the ion exchange polymer only.

^b This value was measured in this study (cf., section 2.3).

^c This value was provided by GE Power and Water.

^d This value was taken from Ref. [10]. It was originally estimated as the average concentration of monovalent counter-ions (i.e., Na^+ , K^+ , Li^+) in the ion exchange polymer, expressed as moles of counter-ions per liter of sorbed water in the ion exchange polymer (after removing the backing contribution), at $C_s = 0.01$ mol/L. The result exhibits excellent agreement with the value reported previously by Kamcev et al. [9].

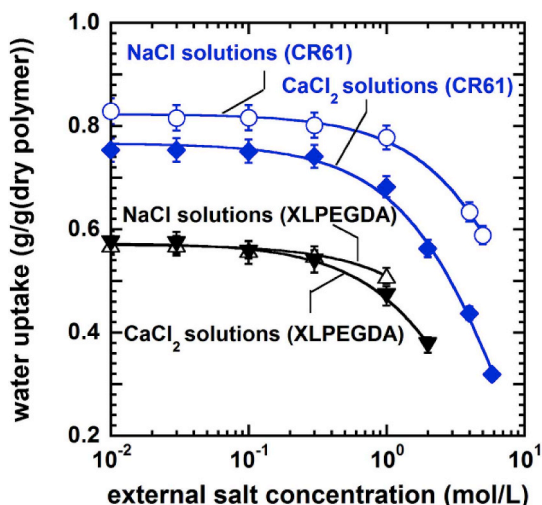


Fig. 1. Water uptake at ambient temperature in CR61 and XLPEGDA as a function of salt concentration in the contiguous external solution. Continuous lines are a guide for the eye.

membranes were gently blotted with paper tissue and soaked in NaCl and CaCl₂ solutions whose concentrations ranged from 0.01 mol/L to 5 mol/L and 6 mol/L, respectively, until reaching ion sorption equilibrium. After 24 h, the membranes were removed from the solutions. Membrane thickness was measured with a micrometer (Mitutoyo Series 293, Aurora, IL), and membrane diameter was measured using a caliper (Fowler Instruments, Boston, MA) and a digital scanner (CanonScan LiDE, model 9622B002). The excess solution on the membrane surface was removed using a clean paper towel. At this point, two different protocols were adopted to measure anion and cation sorption [10].

To measure anion (i.e., co-ion) sorption, each membrane was soaked in a known volume of pure deionized water, and the mobile salt (i.e., chloride and paired sodium or calcium mobile ions) desorbed from the membrane into the external solution. The volume of deionized water used to desorb the mobile salt was 50 mL for membranes previously equilibrated in 0.01 and 0.03 mol/L salt solutions, 100 mL for membranes previously equilibrated in 0.1, 0.3 and 1 mol/L salt solutions, and 200 mL for membranes equilibrated in salt solutions whose concentration was greater than 1 mol/L. Co-ion (i.e., chloride) concentration in the desorption solution was measured using ion chromatography (Dionex 2100, Sunnyvale, CA). Details regarding the experimental protocol and the method used to correct ion sorption data for the backing contribution are reported elsewhere [10,15]. The final co-ion concentration, $C_X^{m,w}$, was expressed as moles of chloride ions per liter of water sorbed in the ion exchange polymer:

$$C_X^{m,w} = \frac{C_X^{m,p}}{\phi_w} \quad (14)$$

where $C_X^{m,p}$ is the concentration in moles of chloride ions per liter of swollen ion exchange polymer, and ϕ_w is the water volume fraction in the ion exchange polymer, calculated from Eq. (13). For alkali chlorides (i.e., NaCl), salt concentration in the polymer, $C_s^{m,w}$, is equal to $C_X^{m,w}$. For alkaline earth chlorides (i.e., CaCl₂), $C_s^{m,w} = \frac{C_X^{m,w}}{2}$ [10].

To measure cation (i.e., counter-ion) sorption, each membrane was removed from the electrolyte solution and quickly wiped with a clean paper towel to remove excess solution on its surface. Each membrane was stored in a petri dish and dried in a vacuum oven at ambient temperature for 24 h. Following drying, each membrane was transferred to a clean porcelain crucible. Crucibles were then placed in a furnace (Fisher Scientific Isotemp 750, Dubuque, IA), and membranes were ashed at 700 °C in air, as reported previously [10,15]. The resulting inorganic ash was dissolved in 15 mL of 2% HNO₃ solution, and

cation (i.e., Na⁺ and Ca²⁺) concentration in the solution was measured using flame absorption spectroscopy (Varian AA240, Victoria, Australia). Details regarding the experimental protocol and the method used to correct ion sorption data for the backing contribution are reported elsewhere [10,15]. The final counter-ion concentration, $C_M^{m,w}$, was expressed in moles of cations per liter of water sorbed in the ion exchange polymer:

$$C_M^{m,w} = \frac{C_M^{m,p}}{\phi_w} \quad (15)$$

where $C_M^{m,p}$ is the concentration expressed in moles of cations per liter of swollen ion exchange polymer [10].

A similar procedure was used to measure ion sorption in the XLPEGDA membranes, except that, since these membranes had no backing, no backing correction was needed for water and ion sorption data.

3. Results and discussion

3.1. Water uptake

Water uptake by CR61, expressed as grams of water per unit mass of dry ion exchange polymer, is reported in Fig. 1 as a function of salt concentration in the external electrolyte solution. The data presented in Fig. 1 were adjusted by removing the contribution of the backing, which does not sorb water and ions [10], so they reflect the water sorbed by the ion exchange polymer only. Water uptake data were reported as the average of several measurements, with an uncertainty of less than 4%. Water uptake in XLPEGDA is also reported for comparison.

As discussed in Ref. [10], the membrane in the divalent counter-ion form contains less water than in the monovalent counter-ion form. At fixed salt concentration in the contiguous external solution, water uptake by IEMs depends on several factors, such as counter-ion concentration, counter-ion hydration, and external osmotic pressure [6,10]. Divalent Ca²⁺ ions (hydration number, $n_h = 5.2$ [6,16], where n_h is the number of water molecules bound to a single cation) are more hydrated than monovalent Na⁺ ions ($n_h = 1.5$ [6,16]) in a styrenic sulfonated CEM [6] so, in principle, the membrane in the Ca²⁺ form should sorb more water than the membrane in the Na⁺ form. However, as discussed later (cf., section 3.2), the Ca²⁺ concentration in the membrane is one half that of Na⁺ [10]. Moreover, CaCl₂ solutions exhibit, especially at high concentrations, greater osmotic pressures than monovalent salt solutions (cf. Fig. S2, Supporting Information), which favors membrane de-swelling [6,10,12,14].

Regardless of the membrane counter-ion form, severe osmotic de-swelling is observed at high external salt concentrations. As reported in Fig. S3, Supporting Information, water activity in the contiguous, external solution decreases with increasing salt concentration, C_s^s , so, according to the Flory-Rehner model [17], membrane water uptake would also decrease. In this study, water activity in the external solution was calculated using the Pitzer model [12]. Membrane osmotic de-swelling ranging from over 30% (in the case of NaCl) to 77% (in the case of CaCl₂) was observed at 4 mol/L external salt concentration.

Water uptake by XLPEGDA from CaCl₂ solutions is reported in Fig. 1. Since XLPEGDA does not have fixed charge groups on its backbone, it sorbs much less water than CR61. Additionally, CR61 and XLPEGDA membranes likely have different cross-link densities, which would also contribute to differences in water uptake [17]. However, due to the presence of the backing, the actual value of the cross-link density for CR61 is not known, and a fundamental investigation of the effects of cross-link density on membrane water uptake was, therefore, beyond the scope of this study. The qualitative behavior of the water sorption isotherm in XLPEGDA is similar to that of the CR61 cation exchange membrane, with significant osmotic de-swelling observed at

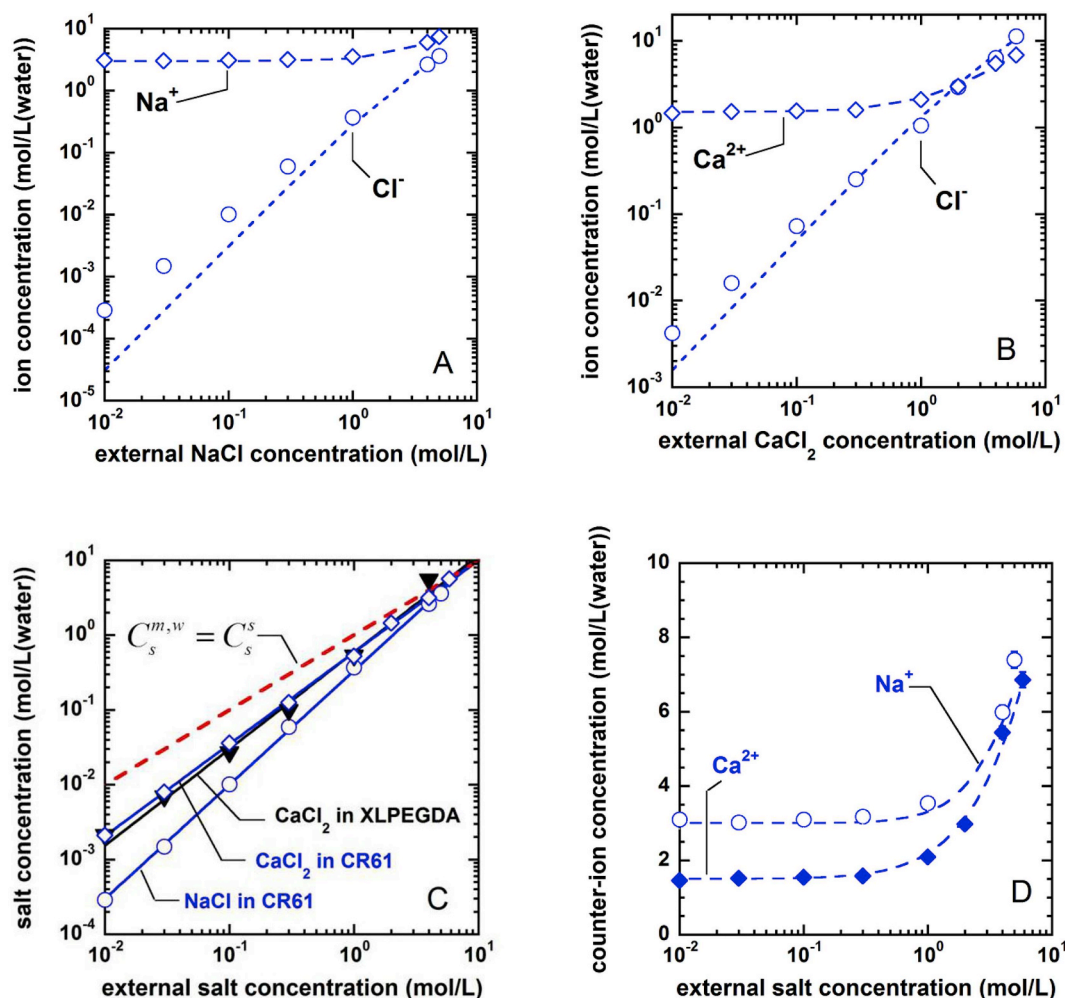


Fig. 2. Co-ion and counter-ion concentration in CR61 as a function of salt concentration in the contiguous external solution. A) NaCl, B) CaCl_2 . The dashed blue lines are predictions from the ideal Donnan model. C) Mobile salt (i.e., co-ion) concentration, $C_s^{m,w}$, in CR61 and XLPEGDA as a function of C_s^s . Blue open circles: NaCl sorption in CR61; blue open diamonds: CaCl_2 sorption in CR61; black filled triangles: CaCl_2 sorption in XLPEGDA. Continuous lines are drawn to guide the eye. The red dashed line represents the parity line, $C_s^{m,w} = C_s^s$. D) Counter-ion concentration in CR61 as a function of C_s^s . Dashed lines are predictions of Eq. (4). Sorption data at $C_s^s \leq 1$ were taken from Ref. [10]. (For interpretation of the references to colour in this figure legend, the reader is referred to the Web version of this article.)

external CaCl_2 concentrations of 1 mol/L and higher. For the sake of comparison, water uptake by XLPEGDA from NaCl solutions was also reported in Fig. 1. At C_s^s values higher than 0.3 mol/L, water sorption from NaCl solutions exceeds that from CaCl_2 solutions, due in part to the higher osmotic pressure exhibited by the CaCl_2 solution.

As confirmed by direct observation under a microscope, CR61 did not exhibit any visible damage upon contact with highly concentrated brines. Similar results were reported by Loeb and co-workers [18] after exposure of a Permeasep P-9 (Dupont) membrane to concentrated NaCl and MgSO_4 solutions.

3.2. Ion sorption

Alkali chloride and alkaline earth chloride sorption data in CR61 up to 1 mol/L external salt concentration were reported previously [10]. In this study, the external concentration range was extended up to 5 mol/L for NaCl and 6 mol/L for CaCl_2 . NaCl and CaCl_2 solubilities in water at 25 °C are 6.1 mol/L and 7.2 mol/L, respectively [19].

In Fig. 2 A–B, ion concentration in CR61, expressed in units of mol of ions per liter of water sorbed in the ion exchange polymer, is reported as a function of salt concentration in the contiguous external solution, C_s^s . The experimental uncertainty is less than 5% for co-ions and less than 3% for counter-ions. Error bars in Fig. 2A–B–C are too small to

show on a log-log scale.

At $C_s^s = 0.01$ mol/L, sodium concentration in CR61 exceeds that of chloride by four orders of magnitude (cf., Fig. 2A). This difference reduces to one order of magnitude at 1 mol/L external salt concentration. Finally, Cl^- and Na^+ concentrations become increasingly similar at $C_s^s = 5$ mol/L. Due to the progressive screening of fixed charge groups by sorbed counter-ions, Donnan exclusion is overwhelmed at high C_s^s (that is, when C_s^s becomes similar to or greater than $C_A^{m,w}$), which ultimately favors co-ion sorption in the membrane [10,15]. In contrast, counter-ion concentration is fairly constant with C_s^s up to $C_s^s = 0.3$ mol/L, since most of cations are sorbed in the membrane to balance the fixed charge groups. At external NaCl concentrations greater than 0.3 mol/L, counter-ion concentration in the ion exchange polymer increases significantly with increasing C_s^s , due to: i) the increase in co-ion sorption, and ii) membrane osmotic de-swelling, which increases the fixed charge density, $C_A^{m,w}$ [10,15].

At $C_s^s = 0.01$ mol/L, calcium concentration in CR61 exceeds that of chloride by 3 orders of magnitude. This difference reduces to less than 1 order of magnitude at 1 mol/L external salt concentration. At $C_s^s = 2$ mol/L, calcium and chloride concentrations in the membrane are essentially the same. Finally, at $C_s^s > 2$ mol/L, calcium and chloride sorption isotherms cross and chloride concentration in CR61 exceeds that of calcium (cf., Fig. 2B). The mobile calcium concentration, $C_{M,mob}^{m,w}$,

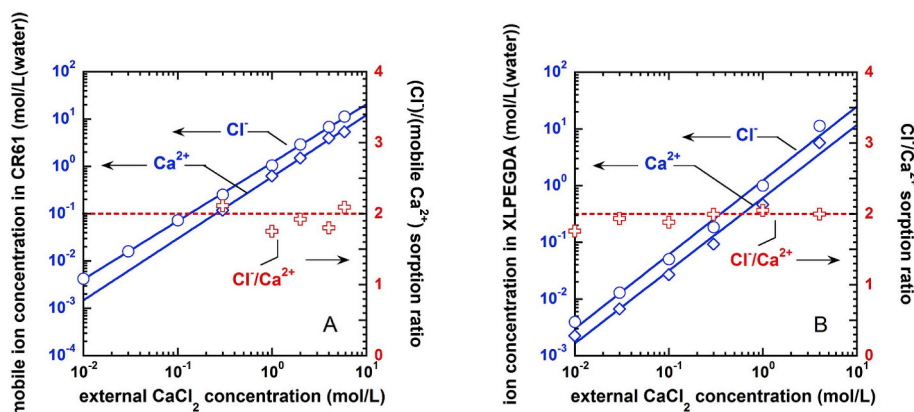


Fig. 3. A) Mobile Ca^{2+} and total Cl^- sorption at ambient temperature in CR61. The total Cl^- -to-mobile Ca^{2+} sorption ratio is reported on the second Y axis. The dashed red line is drawn at $\text{Cl}^-/\text{Ca}^{2+} = 2$. As ion sorption data in IEMs can be inherently inaccurate at $C_s^s \leq 0.03$ mol/L, the calculation of mobile calcium concentration might be affected by a high degree of error, so data at $C_s^s \leq 0.03$ mol/L are not reported. B) Ca^{2+} and Cl^- sorption at ambient temperature in XLPEGDA. The chloride-to-calcium sorption ratio is reported on the second Y axis. The dashed red line is drawn at $\text{Cl}^-/\text{Ca}^{2+} = 2$, which is the expected concentration ratio to satisfy electro-neutrality in the membrane. (For interpretation of the references to colour in this figure legend, the reader is referred to the Web version of this article.)

is readily calculated by subtracting the concentration of fixed counter-ions, which is essentially equal to the total measured calcium concentration at $C_s^s = 0.01$ mol/L, from the total counter-ion concentration measured at different C_s^s values [10]. The concentration of mobile calcium ions sorbed in CR61 is half that of chloride (cf. Fig. 3A) [10], which is required for the membrane to be electrically neutral. In an uncharged hydrogel, such as XLPEGDA, the total sorbed calcium to chloride molar ratio would be 1:2 to satisfy the electro-neutrality condition. As shown in Fig. 3B, experimental data for XLPEGDA are consistent with the required $\text{Cl}^-/\text{Ca}^{2+}$ ratio.

Mobile CaCl_2 concentration in CR61 exceeds that of NaCl by one order of magnitude at moderate external salt concentrations (cf., Fig. 2C), even though the membrane in the calcium counter-ion form contains less water than in the sodium counter-ion form (cf., Fig. 1), and membranes with lower water uptake often sorb less ions [7]. This result can be rationalized considering the Donnan potential, E_D , which is inversely proportional to the counter-ion valence [10]:

$$E_D = -\frac{RT}{z_M F} \ln \left(\frac{\gamma_M^m C_M^{m,w}}{\gamma_M^s C_M^s} \right) \quad (16)$$

where F is the Faraday's constant and the other symbols have the usual meaning. Based on Eq. (16), Donnan exclusion is significantly reduced in the presence of multivalent counter-ions, all other factors being equal, which favors co-ion sorption in the polymer. Thus, in contrast to the behavior typically observed in uncharged hydrogels, where ion sorption can be proportional to membrane water content [20], ion sorption in IEMs, such as CR61, is strongly influenced by electrostatic effects as well [9,10]. NaCl and CaCl_2 mobile salt concentration in CR61 become very similar to one another at $C_s^s > 4$ mol/L (cf., Fig. 2C).

Interestingly, CaCl_2 mobile salt concentrations in XLPEGDA and CR61 are comparable over the entire external concentration range explored (cf., Fig. 2C). Ion sorption in IEMs is strongly influenced by at least two factors: *i*) fixed charge group concentration (i.e., $C_A^{m,w}$), and *ii*) membrane water content [7]. At fixed water content, ion sorption in IEMs decreases with increasing concentration of fixed charge groups, all other factors held constant, due to enhanced Donnan exclusion at high $C_A^{m,w}$ [21]. At fixed charge density, ion sorption in IEMs increases with increasing membrane water content, all other factors being equal [21]. Even though XLPEGDA contains less water than CR61, XLPEGDA does not have fixed charge groups on its backbone, so Donnan exclusion is not operative. We speculate that the two factors mentioned above (i.e., the effects of fixed charge groups and water content) may offset each other, resulting in similar levels of CaCl_2 sorption in XLPEGDA and in CR61. Fundamental studies comparing ion sorption properties of

charged and uncharged materials would be an area for fruitful future studies. In Fig. 2C, the parity line $C_s^{m,w} = C_s^s$ is reported, along with the experimental mobile salt concentration in CR61 and XLPEGDA. Interestingly, at high external salt concentration, NaCl and CaCl_2 concentrations in CR61 become comparable to that in the contiguous, external solution. Likewise, at $C_s^s = 4$ mol/L, CaCl_2 concentration in XLPEGDA matches that in the external solution. This aspect is discussed further in Section 3.3.

Ideal Donnan model predictions of co-ion sorption in CR61 (cf., Eqs. (2) and (4) with $\Gamma = 1$) exhibit large deviations from the experimental data at low to medium values of C_s^s , and good agreement is observed at external concentrations greater than 1 mol/L for NaCl and 0.3 mol/L for CaCl_2 (cf., Fig. 2A and B). To the best of our knowledge, this is the first study where experimental ion sorption data in charged polymers agree with the ideal Donnan model prediction. Fundamental interpretation of this behavior is provided in Section 3.3.

Eq. (4) was used to predict the counter-ion concentration in CR61 [10]. In Eq. (4), co-ion concentration ($C_X^{m,w}$) is calculated from the ideal Donnan model, all other variables being known. The model predictions (which are reported on a more expanded scale in Fig. 2D) exhibit reasonable agreement with the experimental data.

3.3. Ion activity coefficients in the membrane

Co-ion and counter-ion sorption data were used to calculate ion activity coefficients in the membrane, according to Eqs. (7) and (8). In Fig. 4 A-B, ion activity coefficients in CR61 and in the external electrolyte solution are reported as a function of C_s^s . The latter were calculated using the Pitzer model [12].

Ion activity coefficients in solution decrease with increasing C_s^s (cf., dashed lines in Fig. 4A and B) at low C_s^s values. However, at sufficiently high C_s^s values, ion activity coefficients in solution rapidly increase. In contrast, ion activity coefficients in CR61 increase monotonically with increasing C_s^s . This result is consistent with polyelectrolyte theory [13,22–24], which predicts low values of ion activity coefficients at low external salt concentrations, followed by an increase with increasing C_s^s .

As shown in Fig. 4A and B, at low external salt concentrations, ion activity coefficients in CR61 are significantly lower than those in the contiguous external solution. Due to the fixed charge groups, the membrane provides a more thermodynamically favorable environment for counter-ions than the external electrolyte solution. Although ideal Donnan theory assumes that Γ is equal to 1, the data reported in Fig. 4 indicate that, at low external salt concentrations, Γ is much larger than 1 (cf. Fig. S4, Supporting Information). As a result, ideal Donnan model predictions of co-ion sorption in charged polymers exhibit large

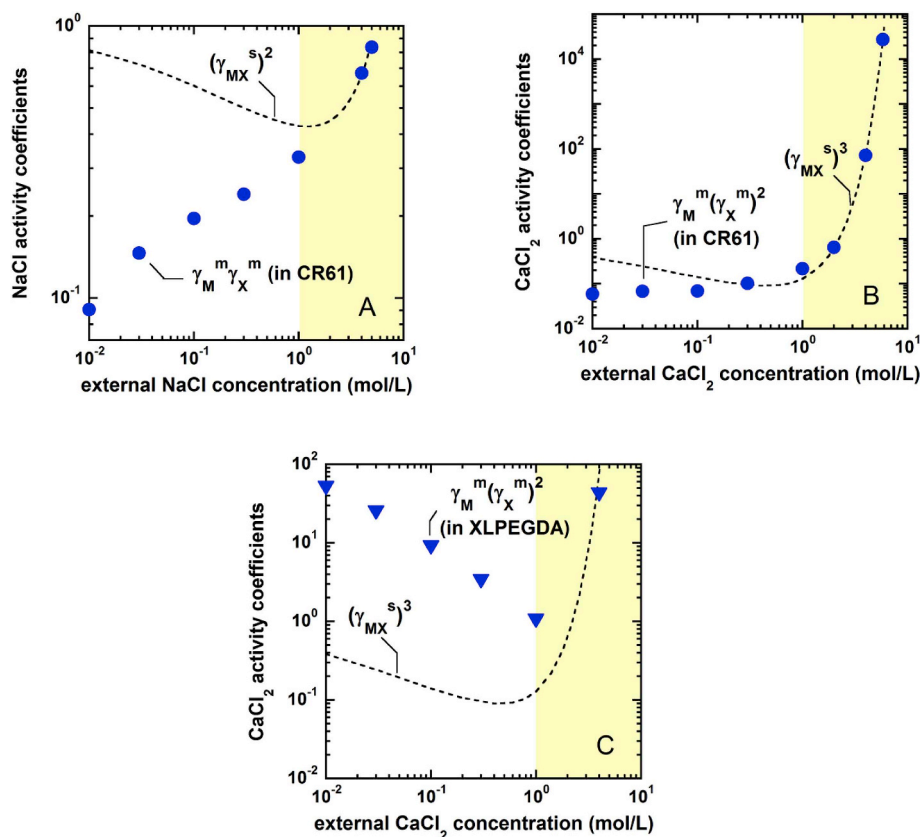


Fig. 4. A) NaCl activity coefficients, $\gamma_M^m \gamma_X^m$, in CR61 as a function of C_s^s , calculated from Eq. (7). B) CaCl_2 activity coefficients, $\gamma_M^m (\gamma_X^m)^2$, in CR61 as a function of C_s^s calculated from Eq. (8). C) CaCl_2 activity coefficients in XLPEGDA, $\gamma_M^m (\gamma_X^m)^2$, as a function of C_s^s calculated from Eq. (8). Blue filled symbols: activity coefficients calculated from experimental ion sorption data using Eqs. (7) and (8); black dashed lines: ion activity coefficients in the external solution, calculated using the Pitzer model [12]. (For interpretation of the references to colour in this figure legend, the reader is referred to the Web version of this article.)

deviations from the experimental data (cf., Fig. 2). For a long time, the validity of the ideal Donnan model to describe ion partitioning between electrolyte solutions and ion exchange polymers was questioned, and alternative models were proposed [25,26]. More recently, the poor agreement between experimental ion sorption data in IEMs and the ideal Donnan model predictions at low external salt concentrations has been ascribed to Γ values being far from 1 [9]. When $C_A^{m,w} \gg C_s^s$, Γ is larger than 1, so corrections for ion non ideal behavior in the membrane and in solution are needed [9,10]. In contrast, when $C_s^s \geq C_A^{m,w}$, Γ is approximately equal to one (cf. Fig. S4, Supporting Information), so the ideal Donnan model provides a reasonable quantitative prediction of ion sorption in charged polymers at high external salt concentrations (cf. Fig. 2). Indeed, when salt concentration in the external solution exceeds 1 mol/L, ion activity coefficients in the CR61 membrane and in solution become similar to one another (cf., Fig. 4A and B). At these conditions, the environment in the membrane becomes thermodynamically similar to that in the external solution. Since most of fixed charges are screened, the membrane environment is essentially made from water and ions [27,28]. This physical picture is further supported by sorption data reported in Fig. 2-C, which show that ion concentration in CR61 and in solution get very close to each other at high C_s^s values.

In Fig. 4C, CaCl_2 activity coefficients in neutral XLPEGDA are reported as a function of C_s^s , along with the values in the external solution. First, CaCl_2 activity coefficients in XLPEGDA are greater than one, and greater than those in solution, which indicates that the solution provides a more thermodynamically favorable environment for ions than the XLPEGDA membrane. In contrast, CaCl_2 activity coefficients in CR61 are less than one at $C_s^s < 1$ mol/L. Unlike in CR61, ion activity coefficients in XLPEGDA and in solution exhibit similar qualitative

behavior over the entire range of external salt concentration considered in this study. Specifically, ion activity coefficients in XLPEGDA and in solution decrease as C_s^s increases to about 1 mol/L, and then increase strongly at higher C_s^s values.

3.4. Manning-Donnan modeling

The Manning-Donnan [9] model requires knowledge of the Manning parameter, ξ , which can be estimated once the distance between fixed charge groups, b , and the dielectric constant of the swollen polymer, ϵ , are known [9,13]. Since the ion exchange polymer in CR61 is believed to be homogeneous, and it does not exhibit any sign of phase separation, fixed charge groups are assumed to be uniformly distributed along the polymer chains [9]. So, the distance between fixed charge groups, b , can be estimated based on the polymer structure and fixed charge concentration, $C_A^{m,w}$ [9]. As explained previously [9], absent any specific experimental information, the dielectric constant of the swollen polymer (i.e., polymer + water) can be estimated as the weighted average of the dry polymer and pure water dielectric constants:

$$\epsilon = \phi_w \epsilon_w + (1 - \phi_w) \epsilon_p \quad (17)$$

where ϕ_w is the water volume fraction in the swollen polymer, which is known from water uptake experiments, and ϵ_w and ϵ_p are the dielectric constants of water and polymer, respectively. As discussed in the literature, ϵ_p values of about 6 provide a reasonable estimate of polymer dielectric constants [9,29]. ϵ_w was assumed to be equal to that of bulk water, i.e., 79 [9].

An important question is whether ξ depends on external salt concentration. Previous studies have shown a weak sensitivity of ξ on C_s^s in the range 0.01–1 mol/L NaCl [9]. So, when C_s^s is less than about 1 mol/

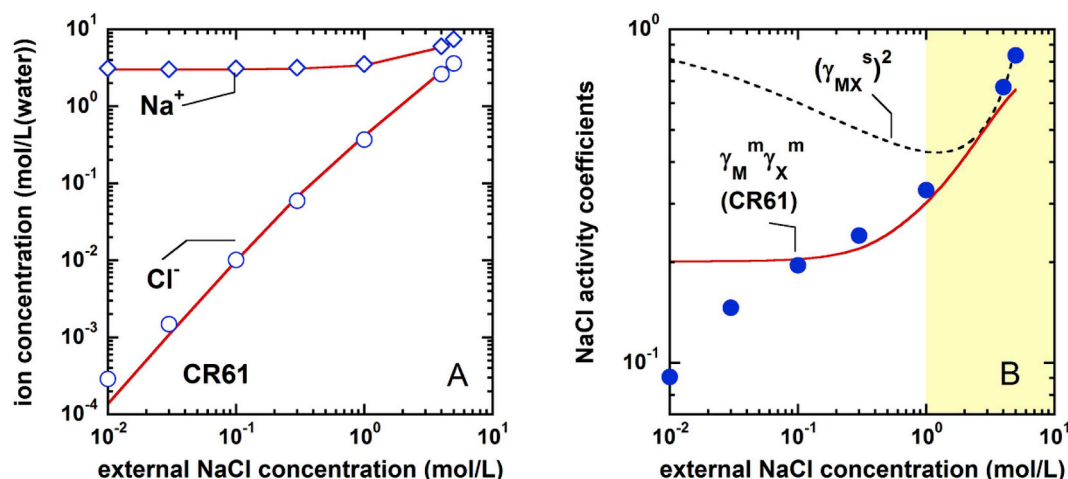


Fig. 5. A) Effect of external NaCl concentration, C_s^s , on Na^+ (blue open diamonds) and Cl^- (blue open circles) concentration in CR61. The red lines represent prediction by the Manning-Donnan model [9]. B) Effect of external NaCl concentration, C_s^s , on NaCl activity coefficients in CR61. Blue filled circles: experimental data; red continuous line: Manning model prediction. Black dashed line: NaCl activity coefficients in the contiguous external solution, calculated using the Pitzer model [12]. (For interpretation of the references to colour in this figure legend, the reader is referred to the Web version of this article.)

L, ξ can be estimated using pure water uptake data. In this study, the external salt concentration was well beyond 1 mol/L in some cases, and water content in CR61 changed appreciably with C_s^s . Since ε enters in the denominator of Eq. (11), a decrease in ε yields an increase in ξ with increasing external salt concentration.

Based on the polymer structure and fixed charge group concentration, the estimated distance between fixed charge groups, b , is 0.73 nm [9]. Using Eq. (17) and pure water sorption data for the membrane in the Na^+ counter-ion form, ε is 42. With these values for b and ε , Eq. (11) gives $\xi = 1.83$ [9].

As shown in Fig. 5A, the Manning-Donnan model provides a reasonable prediction of sodium and chloride concentration in CR61 at C_s^s greater than about 0.03 mol/L. Calculated chloride concentration departs significantly from the experimental data at $C_s^s < 0.03$ mol/L. As discussed previously [9,10], such behavior might be due to a breakdown of one or more of the model assumptions and/or to inherent inaccuracy of ion sorption measurements at low external concentrations. Specifically, the Manning model neglects electrostatic interactions between fixed charge groups on different polymer chains and between fixed ions on the same polymer chain [9]. These assumptions may be less applicable at low external salt concentrations where, due to the very small amount of mobile salt sorbed in the polymer, electrostatic interactions between different chains may not be negligible. Interestingly, the model provides quantitative prediction of NaCl activity coefficients in CR61 (cf., Fig. 5B) at C_s^s values of about 0.1 mol/L or higher. At external salt concentrations greater than 1 mol/L, ion activity coefficients in CR61 are close to those in the contiguous external solution.

The dielectric constant, which is 42 for CR61 at $C_s^s \leq 1$ mol/L, decreases to 36 at $C_s^s = 5$ mol/L. The ξ parameter, which is 1.83 at $C_s^s \leq 1$ mol/L, increases to 2.14 at $C_s^s = 5$ mol/L (cf. Fig. S5, Supporting Information). However, the Manning-Donnan model predictions do not change significantly if ξ is assumed to be equal to 1.83 over the entire external salt concentration range investigated. Specifically, at $C_s^s = 5$ mol/L, the model prediction varies by 1.8% if ξ varies from 1.83 to 2.14. So, the modeling results shown here were based on a constant value of 1.83 for ξ .

In contrast, chloride sorption from CaCl_2 solutions is reasonably predicted at C_s^s values up to about 2 mol/L, with a significant departure from the experimental data observed at $C_s^s > 2$ mol/L (cf., Fig. 6A). As shown in Fig. 4, CaCl_2 activity coefficients in the membrane increase rapidly at $C_s^s > 2$ mol/L and, in this region, they become significantly greater than one. As shown by Eq. (8), the strong increase in $\gamma_M^m(\gamma_X^m)^2$ at

high C_s^s values mirrors the corresponding increase in CaCl_2 activity coefficients in the external solution. The Manning-Donnan model does not allow ion activity coefficients in the membrane to be greater than one, so it cannot capture this behavior. Some authors [30–32] proposed an empirical modification of the original Manning model for a free polyelectrolyte solution with added salt, which can be readily extended to ion exchange polymers. The limiting law derived by Manning [13], which accounts for electrostatic interactions between fixed charge groups on a polyion and small ions, was corrected for Debye-Hückel interactions among mobile ions. Following this approach, ion activity coefficients in IEMs would be expressed as follows [30–32]:

$$[\gamma_M^m(\gamma_X^m)^2]_{\text{mod}} = (\gamma_{MX}^*)^3 [\gamma_M^m(\gamma_X^m)^2] \quad (18)$$

where $[\gamma_M^m(\gamma_X^m)^2]$ is the activity coefficient calculated using Eq. (8), and (γ_{MX}^*) is the mean salt activity coefficient (cf. Eq. (3)) in an aqueous solution whose concentration is $C_s^{m,w}$. (γ_{MX}^*) is calculated using the Pitzer model [12]. Finally, $[\gamma_M^m(\gamma_X^m)^2]_{\text{mod}}$ is the modified Manning activity coefficient. This correction provides an empirical extension of the Manning model to the case of ion activity coefficients in the membrane greater than one. At high salt concentration, the term $[\gamma_M^m(\gamma_X^m)^2]$ calculated from the Manning model reaches its maximum possible value, i.e., one, so $(\gamma_{MX}^*)^3 [\gamma_M^m(\gamma_X^m)^2]$ will almost be equal to $(\gamma_{MX}^*)^3$. As shown in Fig. 6A, the Manning-Donnan model does a good job in predicting CaCl_2 sorption in CR61 at intermediate C_s^s values, with greater deviations from the experimental data observed at $C_s^s > 2$ mol/L. In contrast, when the modified Manning model (cf. Eq. (18)) is plugged into the Donnan model, the resulting modified Manning-Donnan model provides a better prediction at both ends of the external salt concentration range with no adjustable parameters (cf. Fig. 6B). At high external salt concentrations, the vast majority of fixed charge groups are neutralized by divalent counter-ions, and the amount of co-ions sorbed in the membrane is no longer negligible, so the contribution of electrostatic interactions between mobile ions to the Gibbs free energy of the system may no longer be negligible. Consistently, the modified Manning-Donnan model, which takes into account such interactions among mobile ions, provides a better prediction of ion sorption in CR61 at external CaCl_2 concentrations greater than 2 mol/L.

As discussed above, the Manning-Donnan model does not require any correction to describe NaCl sorption in CR61 at high C_s^s values (cf. Fig. 5A), perhaps because mobile salt concentration in the polymer is too small for Debye-Hückel interactions among mobile ions to become important. This hypothesis is supported by NaCl sorption data in

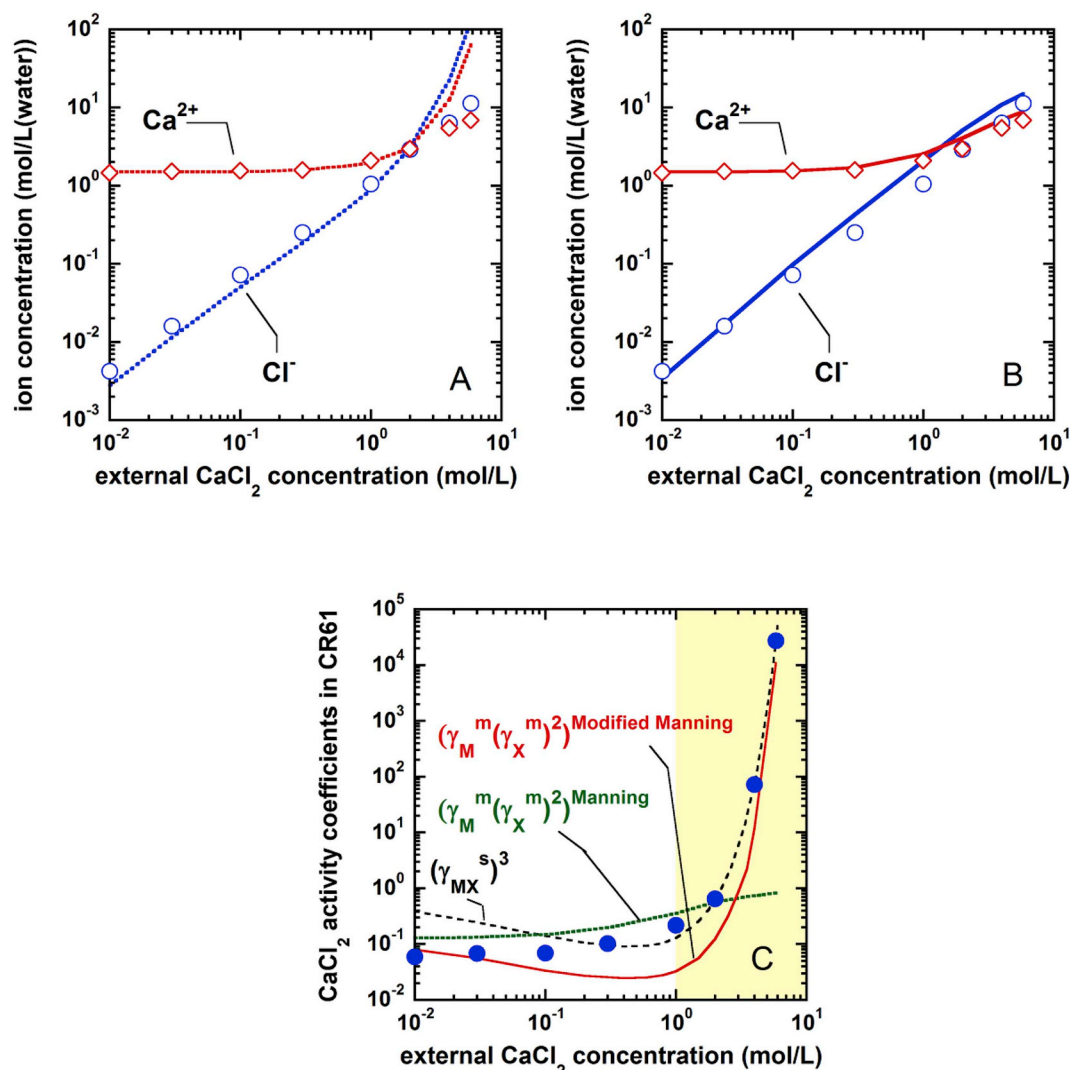


Fig. 6. A) Effect of external CaCl_2 concentration on Ca^{2+} (red open diamonds) and Cl^- (blue open circles) concentration in CR61. The dashed lines represent predictions of the Manning-Donnan model. B) Effect of external CaCl_2 concentration on Ca^{2+} (red open diamonds) and Cl^- (blue open circles) concentration in CR61. The continuous lines represent predictions of the modified Manning-Donnan model. C) CaCl_2 activity coefficients in CR61. Blue filled circles: experimental data; red continuous line: prediction of the modified Manning model; green dotted line: prediction of the Manning model; black dashed line: CaCl_2 activity coefficients in the contiguous external solution. (For interpretation of the references to colour in this figure legend, the reader is referred to the Web version of this article.)

Fig. 2A, where Cl^- concentration in CR61 is still lower than Na^+ concentration even at $C_s^s = 5$ mol/L, which indicates that the membrane CR61 is not completely neutralized.

The experimentally determined and predicted CaCl_2 activity coefficients in the membrane CR61 are compared in Fig. 6C. The modified Manning model significantly improves the prediction of ion activity coefficients in the membrane at both ends of the external salt concentration range, with a worsening observed at intermediate C_s^s values. Since the model correction is empirical, a fundamental interpretation of the deviation observed at intermediate external concentrations is not offered at this time.

Due to the lower water content relative to the membrane in the Na^+ counter-ion form, as well as to strong membrane osmotic de-swelling, the CR61 dielectric constant decreases from 41 to 26, and the ξ parameter increases from 1.83 to 2.95 upon exposure to a 6 mol/L CaCl_2 solution (cf. Fig. S5, Supporting Information). However, if ξ is set equal to 1.83 over the entire C_s^s range investigated, the effect on the accuracy of Manning-Donnan model prediction is little. For example, for CaCl_2 sorption in CR61 at $C_s^s = 6$ mol/L, the model prediction worsens by 0.4% if ξ varies from 2.95 to 1.83. Thus, ξ was set equal to a constant value of 1.83.

The Manning-Donnan model cannot be used to describe ion sorption in XLPEGDA, since this polymer is uncharged and ion activity coefficients in XLPEGDA are larger than one over the entire C_s^s range.

4. Conclusions

The ideal Donnan model was used to predict ion partitioning between concentrated NaCl and CaCl_2 brines and a cation exchange membrane based on cross-linked poly(p-styrene sulfonate-co-divinylbenzene). The model performance is poor at external salt concentration less than 1 mol/L. However, good agreement with experimental ion sorption data is found at external salt concentrations greater than 1 mol/L. Previous studies demonstrated that the poor agreement between the ideal Donnan model predictions and experimental ion sorption data in ion exchange polymers arises from neglecting non-ideal thermodynamic behavior of ions. However, when CR61 is equilibrated with concentrated brines, ion activity coefficients in the membrane and in the external electrolyte solution become similar to one another, so the fundamental Donnan assumption of $\Gamma = 1$ becomes more valid, and the ideal Donnan model provides a good quantitative prediction of NaCl and CaCl_2 sorption in CR61. At high external salt concentrations, the

membrane environment becomes thermodynamically similar to that in the contiguous external solution. The recently developed Manning-Donnan model was used to further validate the experimental findings. An empirical modification of the Manning model was required to describe the experimental CaCl_2 activity coefficients in CR61 at external salt concentration greater than 2 mol/L. When the modified Manning expression for ion activity coefficients in the membrane is plugged into the Donnan model, the resulting modified Manning-Donnan model provides a satisfactory description of CaCl_2 sorption in CR61.

Acknowledgments

This work was supported as part of the Center for Materials for Water and Energy Systems (M-WET), an Energy Frontier Research Center funded by the U.S. Department of Energy, Office of Science, Basic Energy Sciences under Award #DE-SC0019272. The authors wish to thank Dr. N. Moe and Dr. J. Barber from *General Electric Power and Water* for providing the CR61 membrane.

Appendix A. Supplementary data

Supplementary data to this article can be found online at <https://doi.org/10.1016/j.polymer.2019.01.026>.

References

- H. Strathmann, A. Grabowski, G. Eigenberger, Ion-exchange membranes in the chemical process industry, *Ind. Eng. Chem. Res.* 52 (2013) 10364–10379 <https://pubs.acs.org/doi/abs/10.1021/ie4002102>.
- A.E. Childress, M. Elimelech, Effect of solution chemistry on the surface charge of polymeric reverse osmosis and nanofiltration membranes, *J. Membr. Sci.* 119 (1996) 253–268 <https://www.sciencedirect.com/science/article/pii/S0376738896001275>.
- P. Długołęcki, K. Nymeyer, S. Metz, M. Wessling, Current status of ion exchange membranes for power generation from salinity gradients, *J. Membr. Sci.* 319 (2008) 214–222 <https://www.sciencedirect.com/science/article/pii/S0376738808002548>.
- G. Merle, M. Wessling, K. Nijmeijer, Anion exchange membranes for alkaline fuel cells: a review, *J. Membr. Sci.* 377 (2011) 1–35 <https://www.sciencedirect.com/science/article/pii/S0376738811003085>.
- M.R. Singh, E.L. Clark, A.T. Bell, Effects of electrolyte, catalyst and membrane composition and operating condition on the performance of solar driven electrochemical reduction of carbon dioxide, *Phys. Chem. Chem. Phys.* 17 (2015) 18924–18936 <http://pubs.rsc.org/en/content/articlelanding/2015/cp/c5cp03283k/unauth#divAbstract>.
- F. Helfferich, *Ion Exchange*, Dover Publications, New York, 1995.
- G.M. Geise, D.R. Paul, B.D. Freeman, Fundamental water and salt transport properties of polymeric materials, *Prog. Polym. Sci.* 39 (2014) 1–42 <https://www.sciencedirect.com/science/article/pii/S0079670013000804>.
- F.G. Donnan, The theory of membrane equilibria, *Chem. Rev.* 1 (1924) 73–90 <https://pubs.acs.org/doi/abs/10.1021/cr60001a003?journalCode=chreay>.
- J. Kamcev, M. Galizia, F.M. Benedetti, E.S. Jang, D.R. Paul, B.D. Freeman, G.S. Manning, Partitioning of mobile ions between ion exchange polymers and aqueous salt solutions: importance of counter-ion condensation, *Phys. Chem. Chem. Phys.* 18 (2016) 6021–6031 <http://pubs.rsc.org/en/content/articlelanding/2016/cp/c5cp06747b/unauth#divAbstract>.
- M. Galizia, F.M. Benedetti, D.R. Paul, B.D. Freeman, Monovalent and divalent ion sorption in a cation exchange membrane based on cross-linked poly(p-styrene sulfonate-co-divinylbenzene), *J. Membr. Sci.* 535 (2017) 132–142 <https://www.sciencedirect.com/science/article/pii/S0376738816324309>.
- D.R. Paul, Reformulation of the solution-diffusion theory of reverse osmosis, *J. Membr. Sci.* 241 (2004) 371–386 <https://www.sciencedirect.com/science/article/pii/S0376738804004120>.
- K.S. Pitzer, *Activity Coefficients in Electrolyte Solutions*, second ed., CRC Press, Boca Raton, 1991.
- G.S. Manning, Limiting laws and counter ion condensation in polyelectrolyte solutions. I. Colligative properties, *J. Chem. Phys.* 51 (1969) 924–933 <https://aip.scitation.org/doi/abs/10.1063/1.1672157>.
- O.D. Bonner, L.L. Smith, A selectivity scale for some divalent cations on Dowex 50, *J. Phys. Chem.* 61 (1957) 326–329 <https://pubs.acs.org/doi/abs/10.1021/j150549a011?journalCode=jpchax>.
- G.M. Geise, L.P. Falcon, B.D. Freeman, D.R. Paul, Sodium chloride sorption in sulfonated polymers for membrane applications, *J. Membr. Sci.* 423–424 (2012) 195–208 <https://www.sciencedirect.com/science/article/pii/S0376738812006138>.
- E.R. Nightingale, Phenomenological theory of ion solvation. Effective radii of hydrated ions, *J. Chem. Phys.* 63 (1959) 1381–1387 <https://pubs.acs.org/doi/abs/10.1021/j150579a011?journalCode=jpchax>.
- P.J. Flory, J. Rehner, Statistical mechanics of cross-linked polymer networks II. Swelling, *J. Chem. Phys.* 11 (1943) 521–526 <https://aip.scitation.org/doi/abs/10.1063/1.1723791>.
- G.D. Metha, S. Loeb, Performance of Permasep B-9 and B-10 membranes in various osmotic regions and at high osmotic pressures, *J. Membr. Sci.* 4 (1979) 335–349 <https://www.sciencedirect.com/science/article/pii/S0376738800833128>.
- R.H. Perry, D.W. Green, *Chemical Engineers' Handbook*, seventh ed., McGraw-Hill, New York, 1999.
- H. Ju, A.C. Sagle, B.D. Freeman, J.I. Mardel, A.J. Hill, Characterization of sodium chloride and water transport in crosslinked poly(ethylene oxide) hydrogels, *J. Membr. Sci.* 358 (2010) 131–141 <https://www.sciencedirect.com/science/article/pii/S0376738810003261>.
- J. Kamcev, D.R. Paul, B.D. Freeman, Effect of fixed charge group concentration on equilibrium ion sorption in ion exchange membranes, *J. Mater. Chem.* 5 (2017) 4638–4650 <http://pubs.rsc.org/en/content/articlelanding/2017/ta/c6ta07954g/unauth#divAbstract>.
- D.H. Freeman, V.C. Patel, T.M. Buchanan, Electrolyte uptake equilibria with low cross-linked ion-exchange resins, *J. Phys. Chem.* 69 (1965) 1477–1481 <https://pubs.acs.org/doi/abs/10.1021/j100889a007?journalCode=jpchax>.
- M. Nagasawa, M. Izumi, I. Kagawa, Colligative properties of polyelectrolyte solutions. V. Activity coefficients of counter- and by-ions, *J. Polym. Sci.* 37 (1959) 375–383 <https://onlinelibrary.wiley.com/doi/abs/10.1002/pol.1959.1203713208>.
- M. Nagasawa, I. Kagawa, Colligative properties of polyelectrolyte solutions. IV. Activity coefficient of sodium ion, *J. Polym. Sci.* 25 (1957) 61–76 <https://onlinelibrary.wiley.com/doi/abs/10.1002/pol.1957.1202510806>.
- E. Glueckauf, R.E. Watts, The Donnan law and its application to ion exchanger polymers, *Proc. R. Soc. A* 268 (1962) 339–349 <http://rspa.royalsocietypublishing.org/content/268/1334/339.short>.
- E. Glueckauf, R.E. Watts, Non-uniformity of cross-linking in ion-exchange polymers, *Nature* 191 (1961) 904–905 <https://www.nature.com/articles/191904a0>.
- J.S. Mackie, P. Meares, The diffusion of electrolytes in a cation-exchange resin membrane I. Theoretical, *Proc. R. Soc. B* 232 (1955) 498–509 <http://rspa.royalsocietypublishing.org/content/232/1191/498.short>.
- M. Galizia, D.R. Paul, B.D. Freeman, Liquid methanol sorption, diffusion and permeation in charged and uncharged polymers, *Polymer* 102 (2016) 281–291 <https://www.sciencedirect.com/science/article/pii/S0032386116307984>.
- J.C.T. Kwak, Mean activity coefficients for the simple electrolyte in aqueous mixtures of polyelectrolyte and simple electrolyte. System sodium polystyrenesulfonate-sodium chloride, *J. Phys. Chem.* 77 (1973) 2790–2793 <https://pubs.acs.org/doi/abs/10.1021/j100641a015?journalCode=jpchax>.
- J.D. Wells, Thermodynamics of polyelectrolyte solutions. An empirical extension of the Manning theory to finite salt concentrations, *Biopolymers* 12 (1973) 223–227 <https://onlinelibrary.wiley.com/doi/abs/10.1002/bip.1973.360120202>.
- J.C.T. Kwak, M.C. O'Brien, D.A. McLean, Mean activity coefficients for the simple electrolyte in aqueous mixtures of polyelectrolyte and simple electrolyte. The system potassium chloride-potassium poly(styrene sulfonate), magnesium chloride-magnesium poly(styrene sulfonate), and calcium chloride-calcium poly(styrene sulfonate), *J. Phys. Chem.* 79 (1975) 2381–2386 <https://pubs.acs.org/doi/abs/10.1021/j100589a007?journalCode=jpchax>.
- J.C.T. Kwak, R.W.P. Nelson, Mean activity coefficients for the simple electrolyte in aqueous mixtures of polyelectrolyte and simple electrolyte. 4. The system nickel chloride-nickel poly(styrene sulfonate), zinc chloride-zinc poly(styrene sulfonate), and cadmium chloride-cadmium poly(styrene sulfonate), *J. Phys. Chem.* 82 (1978) 2388–2391 <https://pubs.acs.org/doi/abs/10.1021/j100511a008?journalCode=jpchax>.